RSC Sustainability

ROYAL SOCIETY OF CHEMISTRY

COMMUNICATION

View Article Online
View Journal | View Issue

Cite this: *RSC Sustainability*, 2025, **3**, 1339

Received 30th October 2024
Accepted 3rd February 2025

DOI: 10.1039/d4su00679h

rsc.li/rscsus

Direct air capture (DAC): molten carbonate direct transformation of airborne CO_2 to durable, useful carbon nanotubes and nano-onions†

Gad Licht,*[a] Ethan Peltier,[b] Simon Gee[b] and Stuart Licht *[abc]

This study introduces the concept and first demonstration of an effective molten carbonate chemistry for Direct Air Capture (DAC). Molten carbonate electrolysis is a high-temperature decarbonization process within Carbon Capture, Utilization and Storage (CCUS) that transforms chemistry transforming flue gas CO_2 into carbon nanotubes and carbon nano-onions. The key challenge for molten carbonate DAC is to split air's 0.04% CO_2 without heating the remaining 99.6%. This is accomplished by integrating a diffusive, insulating membrane over an electrolyte with a high affinity for CO_2.

Sustainability spotlight

The concept and first demonstration of an effective direct air capture molten carbonate chemistry is presented for removal of the greenhouse gas carbon dioxide to mitigate global warming which is an existential threat to the planet. Molten carbonate electrolysis is an CCUS high-temperature decarbonization chemistry transforming flue gas CO_2 to graphenes. Its direct air capture challenge is to split air's 0.04% CO_2 without heating the remaining 99.6% of the air, which is accomplished here by integration of a membrane over a high CO_2 affinity electrolyte.

Introduction

Direct air capture technologies

Atmospheric Greenhouse gas removal is a necessary component to limit climate change.[1,2] Today's chemical Direct air capture decarbonization technologies[2] typically rely on active CO_2-concentration, often using sorbents such as amine binding, or lime reactions, as described in the ESI.†[3,4] CO_2-concentration is energy-intensive, produces rather than reduces CO_2, and provides just the initial step in Carbon Capture and Storage (CCS) or Carbon Capture, Utilization, and Storage resulting in concentration, rather than storage. In contrast, this demonstration presents an efficient chemical DAC process that eliminates the need for active CO_2 concentration.

C2CNT: transition metal nucleated electrolytic CCUS

We've developed a large-scale transition metal nucleated molten carbonate chemistry to electrolytically split CO_2 into carbon nanotubes (CNTs) and nano-onions (CNOs) and other Graphene NanoCarbon allotropes (GNCs) (ESI Section†). This C2CNT (CO_2 to Carbon Nano Technology) process is highly effective for flue gas decarbonization. Graphite, as a multi-layered graphene, demonstrates the long-term sequestration potential of structures built from graphene. The challenge for C2CNT as a DAC Technology is to efficiently split air's 0.04% CO_2 without heating the remaining 99.96% composition to the ~750 °C of the C2CNT electrolysis. This study presents the concept and first demonstration of an effective DAC molten carbonate chemistry.

CNTs possess the highest tensile strength ever recorded (93 900 MPa) and feature exceptional thermal conductivity, high charge storage, flexibility, and catalytic properties.[5,6] As described in the ESI,† they enhance structural materials such as cement and steel, and are used in a variety of applications including in medical and electrochemical fields, electronics, batteries, supercapacitors, sensing, plastics, textiles, hydrogen storage, and water treatment.

High-temperature molten carbonate electrolytic CO_2-splitting into C and O_2 as a mitigation strategy was first introduced by our group in 2009–2010.[7] By 2015, it was demonstrated that this process could convert CO_2 into valuable, specialized graphene carbons, GNCs, through transition metal nucleated growth.[8–10] The type of useful GNCs, such as CNTs and CNOs produced depends on the electrochemical conditions (ESI†), which offers a promising climate change mitigation approach. The process follows a 4-electron redox reaction of carbonate:

$$CO_3^{2-}(\text{molten}) \rightarrow C(\text{GNC}) + O_2(\text{gas}) + O^{2-}(\text{dissolved}) \quad (1)$$

[a]*Direct Air Capture LLC, A4 188 Triple Diamond Blvd, North Venice, FL 34275, USA. E-mail: slicht@gwu.edu*

[b]*Carbon Corp, 1035 26 St NE, Calgary, AB T2A 6K8, Canada*

[c]*Dept. of Chemistry, George Washington University, Washington DC 20052, USA*

† Electronic supplementary information (ESI) available. See DOI: https://doi.org/10.1039/d4su00679h

The oxide reacts with CO_2 to regenerate carbonate:

$$CO_2(gas) + O^{2-}(dissolved) \rightarrow CO_3^{2-}(molten) \quad (2)$$

These reactions combine to split CO_2 into carbon products and O_2:

$$CO_2(gas) \rightarrow C(GNC) + O_2(gas) \quad (3)$$

The CCUS molten carbonate electrolysis process for CNT and CNO production has evolved into a sophisticated technology. By adjusting the CO_2 electrolysis conditions, specific GNCs can be produced, including doped, thin, thick, long, magnetic, nano-bamboo, and helical CNTs, as well as nano-scaffold, graphene, nano-pearl, and nano-onion morphologies as described in the ESI.†[9,10]

We have explored alternative alkali carbonate mixtures and lower electrolysis temperatures, which can produce 3D-symmetry graphene scaffolds (ESI†). Electrolysis current densities ranging from 0.03–0.6 A cm^{-2} affect GNC growth; higher densities favour the formation of helical CNTs (ESI†). Electrolysis requires a voltage range from 0.8–2 V. Using renewable energy sources can further reduce the CO_2 footprint (ESI†). High purity GNCs form directly on the cathode and are separated from the molten electrolyte through high-temperature filtration, as described in the ESI.†

C2CNT process modules are called the Genesis Device®, and large-scale CCUS Genesis modules transforming the 5% CO_2 flue gas from the Shepard Natural Gas Power Plant are operating in Calgary, Canada. Today, large-scale Genesis electrolysis uses cathodes over 10 000 cm^2. The oxidation resistance of the CNTs produced is high, with a 97.1% TGA purity. SEM and TEM images of the CNT product are detailed in the ESI.† The units tested in this study are bench-top scale, using similar Muntz brass cathodes, 304SS anodes, and 99.5% purity Li_2CO_3 electrolyte. These units are housed in a 12 × 12 × 15 cm carbon pot electrolyzer, which contains the molten electrolyte and serves as the electrolysis chamber, housed within a converted Caldera Paragon kiln. The CO_2- concentration is measured with a CO2meter (**http://co2meter.com/**) sensor situated externally from the hot chamber connected *via* a 304SS tube which allows sufficient cooling to facilitate the room-temperature sensor performance.

C2CNT decarbonization is a unique process, unlike other CCS processes in that it directly (without pre-concentration) transforms CO_2 to high-purity, high-yield GNCs at ~750 °C. This decarbonization process, which eliminates the need for CO_2 concentration, as the electrolyte is a carbon sink that draws in CO_2 with a high affinity, applies to both C2CNT industrial CCUS (Carbon Capture, Utilization and Storage) and C2CNT DAC. However, the feed gas for industrial gas typically ranges from 5% CO_2 (natural gas power plant stack emissions) to over 30% CO_2 (cement plant emissions), and furthermore is generally hot coming off the industrial process. In contrast, DAC utilizes ambient temperature air containing a very low CO_2 concentration. Unlike C2CNT CCUS, DAC may require more energy to heat the entire air feed to >700 °C electrolysis temperatures. Air contains 0.042% CO_2, with the remaining >99.95% consisting of N_2, O_2, H_2O and Ar. While the latter are highly insoluble in molten carbonates, CO_2 dissolves reactively as shown in eqn (2). For effective DAC decarbonization, the C2CNT process energy should not be used to heat the 99.95% non-CO_2 components of air.

The first DAC technology is presented that simultaneously (1) directly (without preconcentration) removes CO_2 from the air, (2) transforms the CO_2 into a valuable product (such as CNTs) provides a strong incentive to remove this greenhouse gas, and (3) unlike previous regular C2CNT processes, insulates the feed air from the hot electrolysis chamber while still allowing CO_2 to diffuse into the electrolysis chamber.

CO_2 diffusion through high temperature insulation

The known diffusion coefficient of CO_2 in air varies as:[11]

$$D_{CO_2}(T_K) = 2.7 \times 10^{-5} {T_K}^{1.59}/e^{(102.1/T_K)} \quad (4)$$

We recently characterized the rate of CO_2 diffusion at room temperature through a variety of high temperature porous insulations acting as membranes.[11] These diffusion results are now used to develop a new high temperature direct air capture, in which these membranes are placed between the feed air and a high-temperature molten electrolyte that removes CO_2 *via* electrolysis in the carbon pot. Insulation materials tend to be porous and low-density. The majority of high-temperature alumina or CaO/MgO silicate insulations we recently studied have densities ranging from 0.06–0.14 g cm^{-3}, with a measured porosity, of ε ranging from 0.89–0.96. Higher density-insulation (0.59 to 0.70 g cm^{-3}) had a measured porosity of $\varepsilon = 0.45$–0.67.[11] As expected, the manufacturer's thermal insulation values tend to vary linearly with thickness and, to a lesser extent, with density. For example, 1/4″ insulation with densities of 0.10 and 0.13 g cm^{-3} have respective *R*-values of 0.3 and 0.4, while 4× thicker insulation has *R*-values of 1.1 to 1.5. Alumina and CaO/MgO silicate insulations had similar *R*-values.

In that room temperature study, we determined that CO_2 readily diffuses through porous ceramic thermal insulators. The measured CO_2 diffusion coefficient for the silicate membranes was found to correlate with the measured open-channel porosity as follows:[11]

$$D_{M\text{-porous-}CO_2} = D_{CO_2} \cdot \varepsilon(M)^{3/2} \quad (5)$$

These diffusion rates were further increased by approximately 50% with turbulent flow (either parallel or perpendicular flow) over the upper membrane surface.[11] These findings, combined with eqn (4) and (5), are now used to configure a DAC C2CNT process that enables the chemical permeation of CO_2 while insulating air's other components from the hot molten carbonate electrolysis.

Experimental section

Electrolyses were conducted using a 750 °C Li_2CO_3 (99.85%, Shanghai Seasongreen Chemical Co.) electrolyte, with or

without a Li_2O additive (99.5% Alfa Aesar), in a 12 × 12 × 15 cm tall 304SS pot and a Muntz brass cathode (Marmetal Industries). In these small-scale experiments, samples were collected from the cooled cathode, and acid-washed to remove electrolyte interspersed with the cooled product. In larger-scale experiments (ESI Section†) the molten electrolyte is directly extracted from the product using high temperature presses.

The Genesis DAC configuration was tested according to the lower left-illustration of Fig. 1 using the 12 × 12 × 15 cm tall 304SS pot. Air is fed into the upper chamber at a low flow rate, proportional to the applied constant electrolysis eqn (8). Higher flow rate conditions (×1.5 and ×2 flow rate) conditions were also investigated.

Two aluminosilicate insulations were used as membranes in this configuration, a 1″ (CeraBlanket 8254870040000) and a 1/4″ (CeraBlanket 825680600200P2), with measured porosities of $\varepsilon = 0.93$ and $\varepsilon = 0.91$, respectively.[11] Each was configured in the 3D open-bottom structure shown in the lower left of Fig. 1 with four 20 × 20 cm walls and a top, providing a total membrane surface area of 2000 cm^2.

Results and discussion

A new C2CNT chemistry for DAC rather than CCUS

Fig. 1 compares Genesis CCUS to the new Genesis DAC decarbonization configuration. CO_2 transfer between the ambient gas feed and the C2CNT electrolysis electrolyte interface is dominated by convection. The placement of the flue gas, exit, CO_2-sensor, and thermocouple placement are illustrated, as well as the external electrical connectors to the anode and cathode. A matrix of GNCs, with interspersed electrolyte grows at the cathode and is periodically lifted to harvest the GNC product.

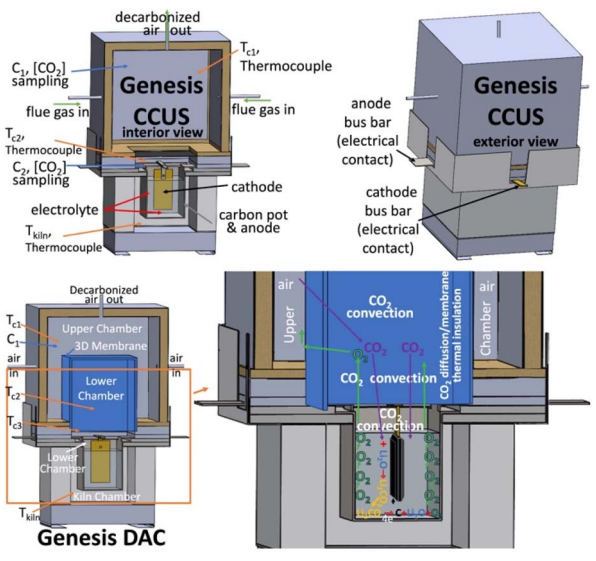

Fig. 1 Active component comparison of the new Genesis DAC for the decarbonization in air, compared to the Genesis CCUS for the decarbonization of flue gas. Both transform CO_2 to GNCs, such as CNTs. (Top) Genesis CCUS interior (left) and exterior view (right) view for decarbonization of flue gas. (Bottom) Genesis DAC for direct air capture including a large 3D membrane separating the air feed and the electrolysis chamber, from an interior view (left) and viewing the decarbonization action (right).

The Genesis DAC configuration in the bottom of Fig. 1 utilizes the recently characterized CO_2 diffusion properties of open-channel porous thermal insulation, and reduces heat loss while sustaining CO_2 transfer between an ambient air feed gas and the interior of the C2CNT electrolysis chamber, which acts as a carbon sink. CO_2-transport in the upper air feed chamber and in both the lower electrolysis chamber are dominated by convection. As illustrated at the bottom portion of Fig. 1, Genesis DAC positions a high-surface area porous insulation as a membrane creating a quiescent zone between the air feed and the electrolysis chamber. In this quiescent zone CO_2 mass transport by diffusion, rather than by convection, dominates. By maintaining a high 3D surface area of this interfacial diffusion zone, sufficient CO_2 enters the electrolysis chamber to replenish the CO_2 consumed.

Sustainable DAC rates and feed gas air flow

The membrane diffusion-limited sustainable CO_2-splitting current, JM_{CO_2}, is determined from $D_{\text{M-porous-CO}_2}$, eqns (4) and (5), and the volume $V(T_K)$ of 1 mole of CO_2 at temperature T_K. JM_{CO_2} has units of mA cm^{-2} when calculated from the CO_2 transported per cm^2 of the membrane, the membrane thickness l_M (cm), the CO_2 $C_o = 0.042\%$ concentration in the air, and Faraday's constant $F = 96\,485$/mole e^-. For the $n = 4e$ CO_2-reduction is then:

$$JM_{CO_2}(T_K, \text{mA cm}^{-2}\text{ membrane}) = 1000 \cdot 4F \cdot C_o D_{\text{M-CO}_2}(T_K) \cdot 1\text{ cm}^2/(l_M \times V_{\text{ideal}}(T_K))$$

where

$$V(T_K) = 22\,414\text{ cm}^3\text{ mole}^{-1} \times T_K/273.15\text{ K} \quad (6)$$

These experiments are constant-current electrolyses at $I_{\text{electrolysis}}$ (A) conducted for a time $t_{\text{electrolysis}}$ (s). This charge passed is then converted to the max moles of CO_2 at 20 °C, which can be split by the $n = 4$-electron electrolysis, $mol_{\text{max-CO}_2}$:

$$mol_{\text{max-CO}_2} = (I_{\text{electrolysis}}\text{ (amps)}/4F) \cdot t_{\text{electrolrysis}}\text{ (s)} \quad (7)$$

This ideal conversion of CO_2 will produce an equal number of maximum moles of carbon and oxygen, *i.e.*, $mol_{\text{max-CO}_2} = mol_{\text{max-C}} = mol_{\text{max-O2}}$. From the respective molar masses, the maximum masses are calculated as $m_{\text{max-CO}_2} = 44.01 \times mol_{\text{max-CO}_2}$; $m_{\text{max-C}} = 12.01 \times mol_{\text{max-CO}_2}$; $m_{\text{max-O2}} = 32.00 \times mol_{\text{max-CO}_2}$. Oxygen ($O_2$) from the electrolysis evolves as a gas, and exits the electrolysis chamber.

The required 20 °C airflow (LPM) per amp of electrolysis charge, f_A, is given by:

$$f_A(\text{LPM/A}) = C_o^{-1} \cdot 1\text{ mol CO}_2 \cdot V_{\text{ideal}}\text{ (298.15 K) (60 s min}^{-1})/4F \quad (8)$$

From eqn (8) f_A is 9 LPM air per A of CO_2 splitting electrolysis.

The Genesis DAC efficiency

Δm_{elec} is the measured mass change of the system during the electrolysis. The maximum Δm_{elec}, corresponding to a DAC efficiency of 100%, represents a full absorption of CO_2, *i.e.* $m_{max\text{-}CO_2} = 44.01 \times mol_{max\text{-}CO_2}$, its conversion to carbonate, and the maximum amount of carbon, *i.e.* $m_{max\text{-}C} = 12.01 \times mol_{max\text{-}CO_2}$. The worst-case scenario occurs when DAC Efficiency = 0%, meaning there is no CO_2 absorption during the electrolysis. In this case, all carbon formed reacts with the O_2 produced and is then released as CO_2; *i.e.* $\Delta m_{elec} = -m_{max\text{-}CO_2}$. The max DAC efficiency (100%) case occurs when all the electrolysis required CO_2 is absorbed during that electrolysis at $I_{electrolysis}$ for $t_{electrolrysis}$, and is converted by the electrolysis, and retained as pure carbon GNC product on the cathode, *i.e.* $\Delta m_{elc} = m_{max\text{-}CO_2}$, while O_2 is evolved. This yields the equation for the molten carbonate direct air capture efficiency:

$$\text{DAC eff (\%)} = 100\%(\Delta m_{elec} + m_{max\text{-}CO_2})/(m_{max\text{-}C} + m_{max\text{-}CO_2}) \quad (9)$$

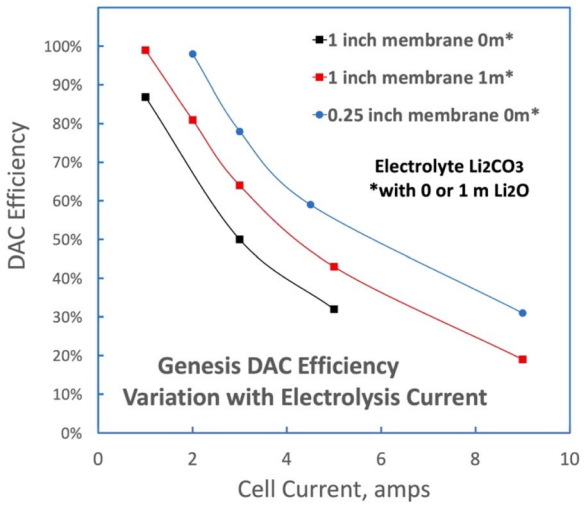

Fig. 2 DAC efficiency as a function of the electrolysis current in DAC Genesis as configured in the lower left of Fig. 1. Black data is measured with eqn (9) required airflow, and red and blue data with 2× higher flow.

Measurement of the genesis DAC efficiency

During electrolysis, the 1-inch thick membrane had an outer surface temperature of 40 °C and an inner surface temperature of 560 °C, providing substantial thermal insulation for the air feed gas, above the hot 750 °C electrolysis chamber. The 1/4-inch membrane offered less insulation, with an outer surface temperature of 160 °C and an inner surface temperature of 450 °C.

The membrane temperature is estimated as the average temperature of its upper and lower surfaces, which is 300 °C for both the 1-inch and 1/4-inch thick membranes The electrochemical current density from eqn (6), JM_{CO_2} (300 °C = 573 K), is 0.67 and 2.5 mA cm^{-2} for the respective 1-inch and 1/4-inch membranes. The $A_{membrane}$ = 2000 cm^2, which multiplied by the area current densities, should support respective electrolysis currents of 1.3 and 5.0 A, respectively.

Fig. 2 presents Genesis DAC Efficiencies from eqn (9) based on the measured mass change, Δm_{elec} at the start and finish of 16 hours 750 °C electrolyses with brass cathodes, and with the carbon pot walls acting as anodes. In the Genesis DAC configuration using a 1-inch insulation as a membrane in the pure Li_2CO_3 electrolyte, a maximum DAC efficiency of 87% was achieved with an electrolysis current of 1 A. However, as shown in the black curve, the efficiency decreases rapidly at higher currents due to insufficient CO_2 reaching the electrolysis chamber.

We have previously noted that in accordance with eqn (2), the addition of 1 m Li_2O increases the rate of CO_2 uptake.[8] At an electrolysis current of 1 A, this addition increases DAC efficiency to 91%. In medium or high airflow (1.5× or 2× the eqn (8) flow), the efficiency rises further to 95% and 99% DAC (red curve). Even with high airflow, however, the DAC efficiency, as shown in the Fig. 2 red curve, decreases again at cell currents >1 A. The systematic increase in cell current (1, 2, 3, 5 and 9 amps) through the 2000 cm^2 surface area membrane demonstrates that DAC efficiency in Fig. 2 decreases with increasing membrane diffusion limited current density. Lower current densities support higher levels of DAC efficiency.

A 1/4-inch membrane supports greater CO_2 diffusion to the electrolysis chamber improving DAC efficiency. This is measured with turbulent (2×) air flow using a pure electrolysis Li_2CO_3 configuration. This configuration supports the highest electrolysis current of 2 A at 98% DAC efficiency, as shown in the Fig. 2 blue curve. Both this, and the 1-inch membrane, measured maximum DAC efficiencies, but these currents occur lower than the calculated eqn (6) supporting currents. The cathode bus bar (seen in Fig. 1) interferes with downward CO_2 flow in the lower chamber and appears to create a bottleneck for CO_2 mass transport to the electrolyte. Future experiments will explore configurations to mitigate this bottleneck, as well as surface-enhanced membranes, such as zig-zag, dimpled and multiple membrane layer designs, which increase the effective membrane area.

The experimental data verifying the accuracy of the theoretical framework is shown in Fig. 3; specifically, the percentage of the applied cell current used for DAC conversion is compared to the theoretical membrane diffusion-limited current:

$$\text{DAC modelled achieved experimentally (\%)} = \text{(DAC efficiency} \times \text{cell current)}/(A_{membrane} \times JM_{CO_2}) \quad (10)$$

As shown in Fig. 3, the product of the modelled membrane-limited rate of CO_2 membrane diffusion limited current, (based on eqns (5) and (6)), generally underestimates the observed DAC capabilities by up to a factor of two, depending on the applied cell current. The observed DAC rate is higher for thinner membranes and tends to increase at higher currents. This two-fold underestimate in the model is a satisfactory preliminary approximation for CO_2 membrane diffusion constants

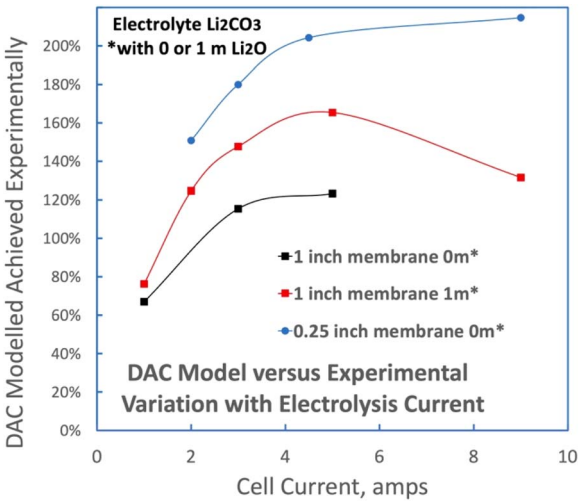

Fig. 3 A comparison of the DAC modelled CO_2 diffusion limited currents and the experimentally measured DAC currents. Black data is measured with eqn (9) required airflow, and red and blue data with 2× higher flow.

measured at room temperature and extrapolated for use with the 750 °C electrolysis of the Genesis DAC configuration. Future studies will explore whether the membrane porosity exponent in eqn (5) $(\varepsilon(M)^{3/2})$ is itself a function of temperature, and the assumption of a linear temperature profile through the membrane's cross section. For example, the results suggest that the lower outer wall temperature of the membrane has a larger effect on the rate of CO_2 diffusion.

CNTs and CNOs products from CO_2 in the air

At 750 °C in Li_2CO_3, the CO_2-splitting electrolysis consistently produces high-purity CNTs as exemplified by the SEM images of the washed product in Fig. 4 panels A & B.

Under CO_2-limiting conditions, where insufficient air CO_2 is fed into the DAC system, an oxide buildup occurs as described by eqn (1) oxide. In this case, we observe that the product tends to be high-purity carbon nano-onions (CNOs) as shown in Fig. 5, panels A through I. When excess CO_2 is reintroduced to the DAC Genesis, CNT production resumes.

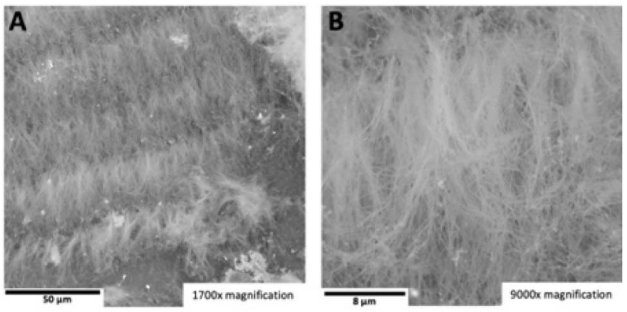

Fig. 4 DAC Genesis CNT products formed at CO_2 sufficient conditions. 750 °C Li_2CO_3 electrolyte electrolysis with a brass cathode and a stainless steel anode and case. SEM of the washed products: CNTs (A & B) 1700× and 9000× magnification.

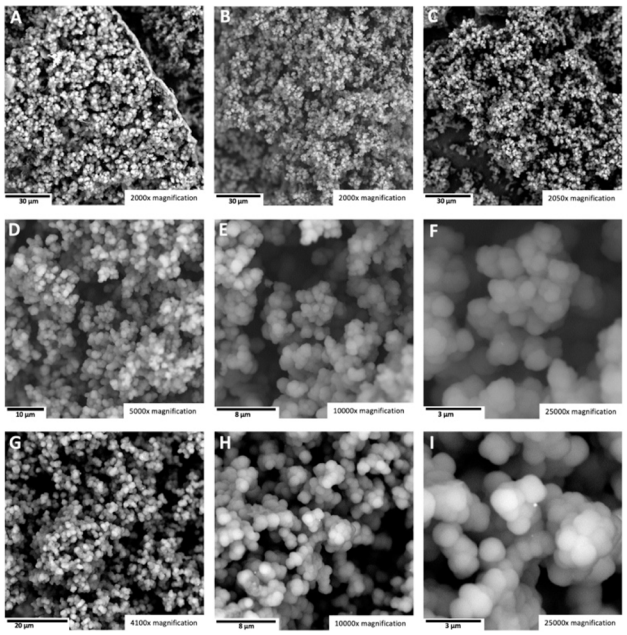

Fig. 5 DAC Genesis CNO products formed at CO_2 insufficient conditions. 750 °C Li_2CO_3 electrolyte electrolysis with a brass cathode and a stainless steel anode and case. SEM of the washed products: CNOs sample 1 (A–F) magnification at 2000×, 2000×, 2050×, 5000×, 100 00×, 250 00×. CNOs sample 2 (G–I) 4100×, 10 000, and 250 00×.

As with CNTs,[12] and as seen in the upper left corner of Fig. 5 (panel A), the CNO growth begins with a thin layer of graphene (observed as removed from the cathode) from which a matrix of CNO growth occurs. Under conditions of insufficient CO_2, higher oxide concentration buildup in the electrolyte, this (i) reduces the solubility and prevalence of transition metal cations in the electrolyte, inhibiting CNT growth by transition metal nucleation, and (ii) induces sp^3 defects in the sp^2 graphene lattice. These sp^3 sites favor the formation of spherical, rather than planar cylindrical, graphene growth.[8,13] Thus, an oxide-rich electrolytic environment promotes CNO over CNT growth.[13]

Alternative graphene nanocarbon products from CO_2 in the air

We have studied the morphology and purity of the GNC products using CO_2 from the air since 2015,[8] although previously without an effective means to separate heat losses between air and the molten electrolyte. In 2016, we demonstrated that using the ^{13}C isotope resulted in the first pure ^{13}C multiwalled carbon nanotube, and tracked the transformation of gas-phased CO_2 into CNTs *via* electrolysis.[14] In 2021, we applied high current density (0.6 A cm^{-2}) and added oxides to the electrolyte, which induced sp^3 defects and torsional effects transforming to CO_2 to helical carbon nanotubes.[15] By controlling electrolysis conditions – including variations in current density, anode, cathode and electrolyte composition, and temperature – we can produce high purity morphologies with a range of properties, including thin-walled, magnetic, doped, nano-bamboo, nano-pearl, and nano-tree CNTs as detailed in the ESI.†[10,12–24]

Alternative electrolytes and an approximation of DAC costs

The CCUS Genesis Device® for decarbonization of flue gas is significantly more mature than the new DAC Genesis Device® for direct air capture. The CCUS electrodes have been scaled up from the original 5 cm^2 area (ref. 8) to over 10 000 cm^2 in electrolysis modules, which comprise 1000 tons of CO_2 decarbonization. These modules are directly fed with 5% CO_2 flue emissions from the adjacent 860 MW Shepard Natural Gas Power Plant in Calgary Canada.[25]

In a recent advancement of the CCUS C2CNT decarbonization chemistry, the majority of the lithium carbonate electrolyte was replaced by strontium carbonate-based electrolytes. The thermodynamic and kinetic chemistry of the electrolytes has been shown to be equivalent for the electrolytic splitting of CO_2 to GNCs. This is economically significant, as strontium salts are an order of magnitude less expensive and considerably more abundant than lithium salts. This shift also alleviates competition for limited lithium carbonate resources which are increasingly used for EVs and grid electric storage. An analysis of C2CNT decarbonization costs based on energy consumption, and the new strontium electrolytes, estimates $198 per tonne of CO_2 ($791 per tonne GNC produced).[25] In that study the equivalent affinities of $SrCO_3$ and Li_2CO_3 for absorbing and releasing CO_2 are demonstrated to be comparable, and are unlike all the other alkali and alkali earth carbonates. The temperature domain in which the CO_2 transformation to GNCs can be effective is <800 °C. Although the solidus temperature of $SrCO_3$ is 1494 °C, it is remarkably soluble in Li_2CO_3 at temperatures less than 800 °C, and the electrolysis energy is low. High purity CNTs are synthesized from CO_2 respectively in $SrCO_3$ based electrolytes containing 30% or less Li_2CO_3. These strontium-based electrolytes are also applicable to the DAC Genesis Device® for direct air capture. The components of DAC and CCUS C2CNT technologies are similar and the additional cost of the porous ceramic diffusion membranes is minor. As a first approximation, the cost per tonne of decarbonization will be similar, and will be analyzed in depth in a subsequent study as the technology is scaled. It is important to note that the C2CNT deployment involves not only the costs mentioned, but also revenue, as GNCs have high value. This provides an additional incentive for DAC C2CNT Genesis deployment.

Conclusions

In conclusion, we have achieved a high rate of CO_2 direct air capture, without requiring active CO_2 concentration. Molten carbonate electrolysis is a powerful method for high-temperature CCUS that converts flue gas CO_2 into GNCs. The main challenge for its DAC counterpart has been extracting CO_2 from air, which contains only 0.04% CO_2, without needing to heat the remaining 99.6% of the air. This study introduces a novel concept and provides the initial demonstration of an effective molten carbonate chemistry for DAC. CO_2 diffuses through high-temperature aluminosilicate insulation, where it is reactively consumed in a molten electrolyte carbon sink and electrolytically transformed into CNTs and CNOs, while the major components of air – N_2, O_2, and H_2O – remain highly insoluble in the electrolyte. Low air feed gas temperatures and moderate electrolysis currents are maintained, ensuring high DAC efficiency.

Data availability

The data supporting this article have been included as part of the ESI.†

Conflicts of interest

There are no conflicts to declare.

Notes and references

1 National Academies of Sciences, Engineering & Medicine, *et al.*, *Negative Emissions Technologies and Reliable Sequestration: A Research Agenda*, National Academies Press, Washington, DC, 2019, DOI: 10.17226/25259.
2 H. Li, *et al.*, Capturing carbon dioxide from air with charged-sorbents, *nature*, 2024, **630**, 654–659.
3 G. Zhang, J. Liu, J. Qian, X. Zhang and Z. Liu, Review of research progress and stability studies of amine-based biphasic absorbents for CO2 capture, *J. Ind. Eng. Chem.*, 2024, **134**, 28–50.
4 Y. Tan, W. Liu, X. Zhang, W. Wei and S. Song, Conventional and optimized testing facilities of calcium looping process for CO_2 capture: A systematic review, *Fuel*, 2024, **358**, 130337.
5 C.-C. Chang, H.-K. Hsu, M. Aykol, W. Hung, C. Chen and S. Cronin, A New Lower Limit for the Ultimate Breaking Strain of Carbon Nanotubes, *ACS Nano*, 2010, **4**, 5095–5100.
6 A. Islam, M. Hasan, M. Rahman, H. Mobarak, M. A. Mimona and N. Hossain, Advances and significances of carbon nanotube applications, *Eur. Polym. J.*, 2024, **2024**, 113443.
7 S. Licht, B. Wang, S. Ghosh, H. Ayub, D. Jiang and J. Ganley, New solar carbon capture process: STEP carbon capture, *J. Phys. Chem. Lett.*, 2010, **1**, 2363–2368.
8 J. Ren, F.-F. Li, J. Lau, L. Gonzalez-Urbina and S. Licht, One-pot synthesis of carbon nanofibers from CO_2, *Nano Lett.*, 2015, **15**, 6142–6148.
9 X. Wang, X. Liu, G. Licht, B. Wang and S. Licht, Exploration of alkali cation variation on the synthesis of carbon nanotubes by electrolysis of CO_2 in molten carbonates, *J. CO_2 Util.*, 2019, **18**, 303–312.
10 X. Liu, G. Licht, X. Wang and S. Licht, Controlled Growth of Unusual Nanocarbon Allotropes by Molten Electrolysis of CO_2, *Catalysts*, 2022, **12**, 137.
11 G. Licht, E. Peltier, S. Gee and S. Licht, Facile CO_2 diffusion for decarbonization through thermal insulation membranes, *DeCarbon*, 2024, **5**, 100063.
12 M. Johnson, J. Ren, M. Lefler, G. Licht, J. V. X. Liu and S. Licht, Carbon nanotube wools made directly from CO_2 by molten electrolysis: Value driven pathways to carbon dioxide greenhouse gas mitigation, *Mater. Today Energy*, 2017, **5**, 230–236.

13 X. Liu, J. Ren, G. Licht, X. Wang and S. Licht, Carbon nano-onions made directly from CO_2 by molten electrolysis for greenhouse gas mitigation, *Adv. Sustainable Syst.*, 2019, **3**, 1900056.
14 J. Ren and S. Licht, Tracking airborne CO_2 mitigation and low cost transformation into valuable carbon nanotubes, *Sci. Rep.*, 2016, **6**, 27760.
15 X. Liu, G. Licht and S. Licht, The green synthesis of exceptional braided, helical carbon nanotubes and nanospiral platelets made directly from CO_2, *Mater. Today Chem.*, 2021, **22**, 100529.
16 X. Wang, X. Liu, G. Licht, B. Wang and S. Licht, Exploration of alkali cation variation on the synthesis of carbon nanotubes by electrolysis of CO_2 in molten carbonates, *J. CO_2 Util.*, 2019, **18**, 303–312.
17 G. Licht, X. Wang, X. Liu and S. Licht, CO_2 Utilization by Electrolytic Splitting to Carbon Nanotubes in Non-Lithiated, Cost-Effective, Molten Carbonate Electrolytes, *Adv. Sustainable Syst.*, 2022, 10084.
18 H. Wu, Z. Li, D. Ji, Y. Liu, L. Li, D. Yuan, Z. Zhang, J. Ren, M. Lefler, B. Wang and S. Licht, One-pot synthesis of nanostructured carbon materials from carbon dioxide via electrolysis in molten carbonate salts, *Carbon*, 2016, **106**, 208–217.
19 X. Wang, G. Licht, X. Liu and S. Licht, One pot facile transformation of CO_2 to an unusual 3-D nano- fold morphology of carbon, *Sci. Rep.*, 2020, **10**, 21518.
20 X. Liu, G. Licht and S. Licht, Controlled Transition Metal Nucleated Growth of Carbon Nanotubes by Molten Electrolysis of CO_2, *Catalysts*, 2022, **12**, 137.
21 X. Wang, F. Sharif, X. Liu, G. Licht, M. Lefler and S. Licht, Magnetic carbon nanotubes: Carbide nucleated electrochemical growth of ferromagnetic CNTs, *J. CO_2 Util.*, 2020, **40**, 101218.
22 M. Johnson, J. Ren, M. Lefler, G. Licht, J. Vicini and S. Licht, Data on SEM, TEM and Raman spectra of doped, and wool carbon nanotubes made directly from CO_2 by molten electrolysis, *Data Br.*, 2017, **14**, 592–606.
23 J. Ren, M. Johnson, R. Singhal and S. Licht, Transformation of the greenhouse gas CO_2 by molten electrolysis into a wide controlled selection of carbon nanotubes, *J. CO_2 Util.*, 2017, **18**, 335–344.
24 X. Liu, X. Wang, G. Licht and S. Licht, Transformation of the greenhouse gas carbon dioxide to graphene, *J. CO_2 Util.*, 2020, **36**, 288–294.
25 G. Licht, K. Hofstetter, X. Wang and S. Licht, A new electrolyte for molten carbonate decarbonization, *Commun. Chem.*, 2024, **7**, 211.